EPJ Web of Conferences **291**, 01004 (2024) https://doi.org/10.1051/epjconf/202429101004
MESON 2023

The BGOOD experiment at ELSA, exotic structures in the light quark sector?

Thomas Jude[1,*], *Alessandro* Braghieri[2], *Philip* Cole[3], *Daniel* Elsner[1], *Rachele* Di Salvo[4], *Alessia* Fantini[4,5], *Antonio Joao Clara* Figueiredo[1], *Oliver* Freyermuth[1], *Frank* Fromberger[1], *Francesco* Ghio[6,7], *Johannes* Groß[1], *Katrin* Kohl[1], *Paolo* Levi Sandri[8], *Guiseppe* Mandaglio[9,10], *Paolo* Pedroni[2], *Mariia* Romaniuk[11], *Georg* Scheluchin[1], *Hartmut* Schmieden[1], and *Adrian* Sonnenschein[1]

[1]Rheinische Friedrich-Wilhelms-Universität Bonn, Physikalisches Institut Bonn, Germany.
[2]INFN sezione di Pavia, Pavia, Italy.
[3]Lamar University, Department of Physics, Beaumont, Texas, USA.
[4]Università di Roma "Tor Vergata", Dipartimento di Fisica, Rome, Italy.
[5]INFN Roma "Tor Vergata", Rome, Italy.
[6]INFN sezione di Roma La Sapienza, Rome, Italy.
[7]Istituto Superiore di Sanità, Rome, Italy.
[8]INFN - Laboratori Nazionali di Frascati, Frascati, Italy.
[9]INFN sezione Catania, Catania, Italy.
[10]Università degli Studi di Messina, Dipartimento MIFT, Messina, Italy.
[11]Institute for Nuclear Research of NASU, Kyiv, Ukraine.

Abstract. The BGOOD photoproduction experiment accesses forward meson angles and low momentum exchange kinematics in the *uds* sector, which may be sensitive to molecular-like hadron structure. Recent results are presented, including strangeness photoproduction at forward meson angles, and $\pi^0\pi^0$ coherent photoproduction off the deuteron.

1 Introduction

Exotic, multi-quark states beyond valence three-quark and quark-antiquark systems are now unambiguously realised in the heavy, charmed quark sector. Many of these states, such as the P_C pentaquarks [1] and XYZ mesons [2] reside close to open charm thresholds, indicative of molecular-like structure. Equivalent structures may also be evidenced in the light, *uds* sector, including the $\Lambda(1405)$ and a cusp-like structure in $K^0\Sigma^+$ photoproduction at the $K^*\Sigma$ threshold [3] which was suggested to derive from a vector meson-baryon dynamically generated state, the $N^*(2030)$ [4]. As described by the Weinberg *Composite Criterion* which defined molecular systems based upon the deuteron [5], such states would be expected to have small binding energy between the constituents and therefore dissociate under large momentum transfer. Experimentally, access to a low momentum exchange region is therefore mandatory to elucidate the role of such states in reaction mechanisms. In a photoproduction experiment with a fixed target, this corresponds to forward meson acceptance to ensure the recoiling hadron system has minimal momentum transfer. The BGOOD experiment [6] at the

*e-mail: jude@physik.uni-bonn.de

ELSA electron accelerator facility [7] is ideally suited for this. A 3 GeV electron beam impinges upon a thin radiator to produce an energy tagged bremsstrahlung photon beam which is subsequently incident upon the target at the centre of the BGOOD experiment. BGOOD is comprised of two main parts, a central calorimeter region ideal for the reconstruction of neutral mesons via their decays, and a forward spectrometer used for charged particle identification and momentum reconstruction at forward angles.

The physics programme at BGOOD is currently focussed on two areas: strangeness photoproduction, with an emphasis on the role of exotic candidates in the reaction mechanism (Sec. 2), and coherent meson photoproduction of the deuteron at forward angles (Sec. 3).

2 Strangeness photoproduction at BGOOD

BGOOD has an extensive strangeness photoproduction physics programme [8–11], with an emphasise on studying reactions at low momentum transfer (low t). Recent results are highlighted in this section.

2.1 The $\gamma n \to K^0\Sigma^0$ differential cross section over the K^* threshold [8]

A model by Ramos and Oset suggested a dynamically generated $N^*(2030)$ amplified a cusp measured in the $K^0\Sigma^+$ channel [3, 4]. The model also predicted constructive interference in $K^0\Sigma^0$ photoproduction resulting in a peak. Observing this experimentally would therefore be direct evidence of a molecular state in the *uds* sector.

An example of the differential cross section measured at BGOOD is shown in Fig. 1. The data are in reasonable agreement with the previous data from the A2 collaboration [12] and in the more forward interval shown, are consistent with the predicted peak from the model of Ramos and Oset. Further data has now been taken to improve the statistical precision and enable a firm interpretation.

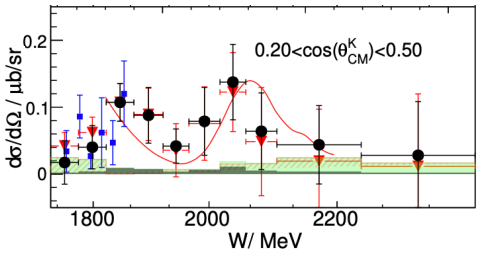

Figure 1. $\gamma n \to K^0\Sigma^0$ differential cross section for $0.2 < \cos\theta^K_{\mathrm{CM}} < 0.5$ and two different fitting methods (red triangles and black circles). The blue squares are data from the A2 Collaboration [12]. The predicted total cross section from Ramos and Oset [4] is included at an arbitrary scale. Figure adapted from Ref. [8].

-

2.2 Photoproduction of $K^+\Lambda(1405) \to K^+\pi^0\Sigma^0$ [9]

Shown in Fig. 2 (left), Ref. [13] proposes that a triangle singularity contributes to the $K^+\Lambda(1405)$ photoproduction, where the "legs" of the triangle are almost on shell, resulting in an enhancement at a centre-of-mass energy of 1900 MeV. This singularity is driven by the same dynamically generated $N^*(2030)$ resonance suggested in $K\Sigma$ photoproduction. If this is proven to be correct, the mechanism supports the molecular-like structure of the $N^*(2030)$ as it must reside close to the $K^*\Sigma$ threshold and have a strong coupling to the open strange system.

Figure 2 (right) shows the cross section versus photon beam energy measured at BGOOD, integrated over all $\cos\theta^K_{\rm CM}$, with good agreement to previous CLAS data and with improved beam energy resolution. The purple line is the calculation by Wang *et al.* of the triangle singularity being driven by the $N^*(2030)$ resonance [13]. The excellent agreement supports the description of a molecular-like $N^*(2030)$ driving a triangle singularity.

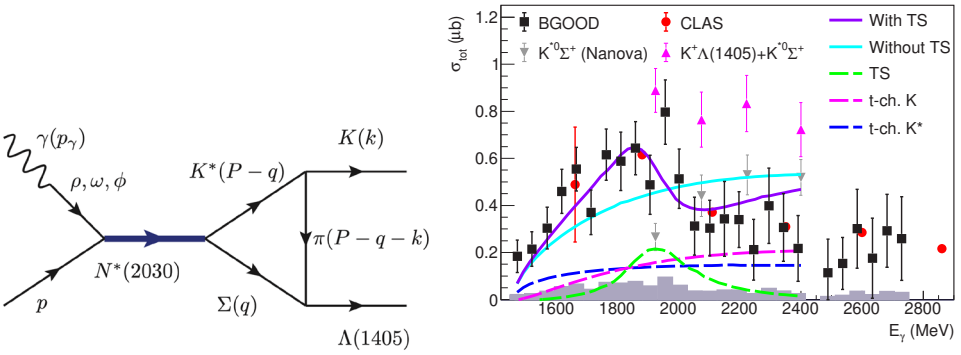

Figure 2. Left: The triangle singularity proposed to contribute to $K^+\Lambda(1405)$ photoproduction. Figure from Ref. [13]. Right: The integrated $\gamma p \to K^+\Lambda(1405)$ cross section. The purple and cyan line is the model of Wang *et al.* [13] with and without the triangle singularity, the $K^{*0}\Sigma^+$ data from CBELSA/TAPS are the grey triangles and the sum of the $K^{*0}\Sigma^+$ and the BGOOD $K^+\Lambda(1405)$ data are the magenta triangles. Red circles are CLAS data. Figure and references of other datasets are in Ref. [9].

2.3 $K^+\Sigma^0$ photoproduction at forward angles and low momentum transfer [10, 11]

$K^+\Lambda$ and $K^+\Sigma^0$ differential cross sections for $\cos\theta^K_{\rm CM} > 0.9$ have both been measured at BGOOD with high statistical precision [10, 11]. The $K^+\Sigma^0$ differential cross section is shown in Fig. 3 (left). A cusp-like structure is resolved close to the pK^+K^- threshold at $W \sim 1900$ MeV. Figure 3 (right) shows the data extrapolated to minimum momentum transfer, $t_{\rm min}$ and $\cos\theta^K_{\rm CM} = 1$, where the cross section drops by 75 %. It is interesting to note the proximity of multiple thresholds and predicted bound states immediately at this centre-of-mass energy. The extent of this cusp-like structure changes quickly over $\cos\theta^K_{\rm CM}$ at forward angles, demonstrating the importance of accessing these forward kinematics.

It is speculated that there appears an equivalence of exotic state candidates observed in these strangeness photoproduction data compared to the P_C states. As outlined in the introduction, the proximity of the states to open charm (see for example the description in Ref. [23]), or in this case strange thresholds supports a molecular description. The $P_C(4457)$ is at the $\Sigma_C\bar{D}^*$ threshold, and at the Σ^0K^{*+} threshold is the proposed $N^*(2030)$ observed as a peak or cusp in $K^0\Sigma$ photoproduction and a candidate for driving a triangle singularity in the $K^+\Lambda(1405)$ final state. The $P_C(4382)$ is at the $\Sigma^*\bar{D}$ threshold. The cusp in the $K^+\Sigma^0$ differential cross section shown in Fig. 3 (right) could be regarded as a peak exactly at the $\Sigma(1385)K^+$ threshold. The $P_C(4312)$ with $J^P = 1/2^-$ is at the $\Sigma_C\bar{D}$ threshold, and the well known $N^*(1535)$ is at the Σ^0K threshold. The large coupling to the ηN final states supports strange quark content, and the resonance has successfully been described previously as dynamically generated using models based on chiral perturbation theory (see for example Ref. [22]). These comparisons are listed in table 1.

Further data is being taken and analysed of other open strangeness final states to further elucidate the roles of candidate exotic states in the *uds* sector.

	Charm sector		Strange sector	
J^P	Threshold	State	Threshold	Evidence
$\frac{1}{2}^-$	$\Sigma_c\bar{D}$	$P_C(4312)$	Σ^0K^+	$N(1535)$?
$\frac{3}{2}^-$	$\Sigma_c^*\bar{D}$	$P_C(4382)$	$\Sigma^0(1385)K^+$	Peak in $K^+\Sigma^0$ [11]
$\frac{3}{2}^-$	$\Sigma_c\bar{D}^*$	$P_C(4457)$	Σ^0K^{*+}	Peak in $K^0\Sigma^0$ [8], Cusp in $K^0\Sigma^+$ [3], Triangle singularity in $K^+\Lambda(1405)$ [9]

Table 1. Comparison between P_C states and their proximity to thresholds to $K\Sigma$ thresholds and evidence of molecular states. The $P_C(4382)$ is a suggestion from Du *et al.* [23].

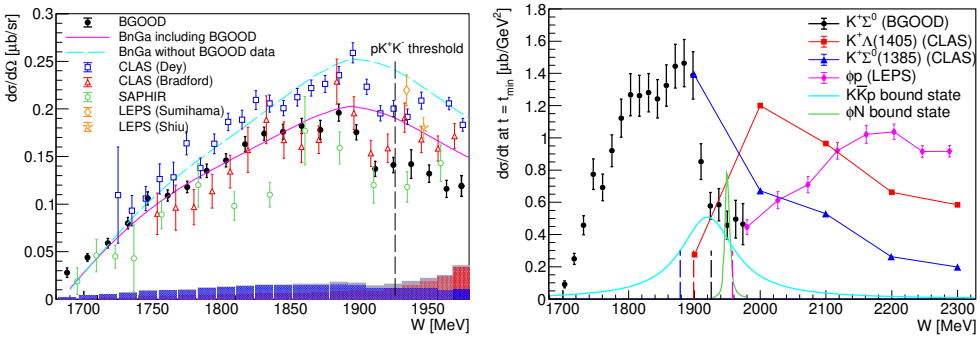

Figure 3. Left panel: $\gamma p \to K^+\Sigma^0$ differential cross section for $\cos\theta^K_{\rm CM} > 0.90$ (black circles). The systematic uncertainties on the abscissa are in three components, where the grey bars are the total. Previous data (only including statistical errors) and model calculations are indicated in the legend. The CLAS data are at the more backward angle of $0.85 < \cos\theta^K_{CM} < 0.95$. Right panel: $d\sigma/dt$ extrapolated to $t_{\rm min}$ versus W (filled black circles). Previous data of other final states indicated in the legend. The vertical dashed lines indicate the respective thresholds, with the addition of the K^+K^-p threshold indicated by the black dashed line. Predictions of $K\bar{K}N$ and ϕN bound states are shown. Figures and references from Ref. [11].

3 Coherent photoproduction of the deuteron at BGOOD [14]

A renaissance in the search for dibaryon states began with the discovery/confirmation of the $d^*(2380)$ in the isoscalar ($I = 0$) channel [15, 16]. The $d^*(2380)$ may have first been observed indirectly earlier in the 1960s via low mass enhancements in $\pi\pi$ invariant mass spectra [17] from deuteron formation in pn reactions, which was also evidenced recently at the WASA collaboration [16].

The reaction $\gamma d \to \pi^0\pi^0 d$ is an ideal channel to search for dibaryons as the isoscalar final state is only sensitive to intermediate isoscalar dibaryons, compared to $\gamma d \to \pi^+\pi^- d$ which also has isovector coupling and background contributions from the large $\gamma N\pi^\pm$ coupling. The reaction was identified at BGOOD via the two $\pi^0 \to \gamma\gamma$ in the BGO Rugby Ball and the deuteron identified in the Forward Spectrometer. The differential cross section for $\cos\theta^d_{\rm CM} > 0.8$ is shown in Fig. 4 (left). The data peaks at $W \sim 2650$ MeV with a cross section of

4 nb/sr. This is approximately an order of magnitude higher than the model prediction of Fix, Arenhövel and Egorov [18, 19] which assumed coherent production off the deuteron, where at forward angles the cross section falls very quickly due to the increasing momentum transfer. At W = 2300 and 2800 MeV, the three-momentum transfer to the deuteron is 0.4 and 1.0 GeV/c respectively, which is much higher than the Fermi momentum of the constituent nucleons (typically 80 MeV/c) and therefore what can be transferred to the deuteron for it to remain intact.

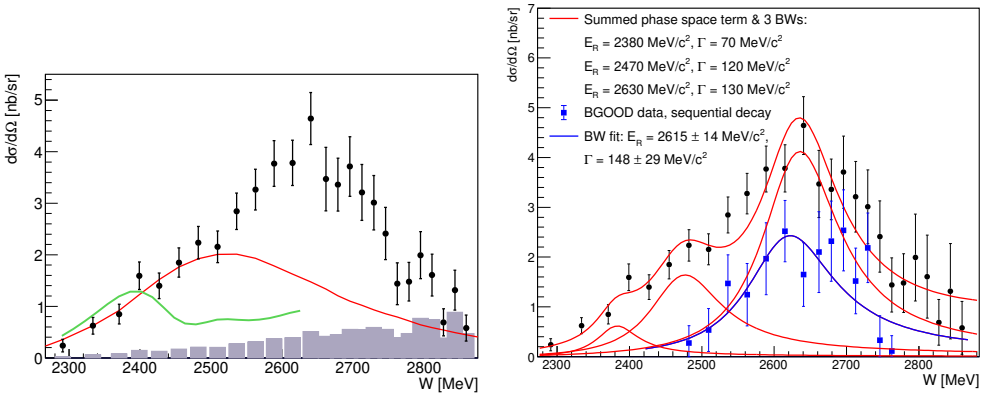

Figure 4. Left: $\gamma d \rightarrow \pi^0\pi^0 d$ differential cross section for $\cos\theta^d_{\rm CM} > 0.8$. The systematic errors are the grey bars on the absisca. The green line is the coherent reaction model of Fix, Arenhövel and Egorov [18, 19] scaled by a factor of five for visibility. The red line is the *Toy Pickup model* described in the publication. Right: The same data where the error bars are the statistical and systematic uncertainties summed quadratically. A fit including three Breit-Wigner functions (BW) are shown as the red lines, with the fixed masses and widths labelled inset. The blue square data points are the differential cross section for the first of the sequential dibaryon candidate determined from the $\pi^0 d$ invariant mass distributions (an example of which is shown in fig. 5(b)) with a Breit-Wigner function fitted and the mass and width labelled inset. Figures from Ref. [14].

Fig. 4 (right) shows the same data fitted with the $d^*(2380)$ and the two additional isoscalar dibaryons reported by the ELPH collaboration [20]. A Breit-Wigner function is assumed for each dibaryon candidate, with masses and widths fixed from Ref. [20] but not their relative amplitudes. The fit is consistent with the three dibaryon scenario however with limited statistical precision and resolution in W.

Figure 5(a) shows the invariant mass of the $\pi^0\pi^0$ system for a W range over the $d^*(2380)$. The low mass enhancement and a dip at approximately 0.34 GeV/c^2 appears similar to the ABC effect in Refs. [15, 16] which was attributed to the $d^*(2380)$. The pink line (scaled to match the data at 0.29 GeV/c^2) shows the expected distribution, where an intermediate $d^*(2380)$ is formed [21]. Qualitatively there is a good agreement over the low mass range below 0.35 GeV/c^2 and is preferred over the phase space spectrum, despite limited statistical precision. A fit was made to the data including this "ABC spectrum" and a differential cross section for $\gamma d \rightarrow d^*(2380) \rightarrow \pi^0\pi^0 d$ was determined as $(17 \pm 7_{\rm stat} \pm 4_{\rm sys})$ nb/sr. With improved statistics, this fitting method can enable a particularly accurate $d^*(2380)$ photoproduction cross section determination.

Figure 5(b) shows the invariant mass of the $\pi^0 d$ system for W = 2641 - 2696 MeV. A double peaking structure is observed which is similar to what was observed by the ELPH Collaboration [20], where it was interpreted as an isovector dibaryon with a mass of 2140±11 MeV/c^2

and a width of 91 ± 11 MeV/c^2 from the decay of an isoscalar dibaryon. This reaction mechanism was input to the BGOOD simulation where the mass and width was varied to achieve a minimal χ^2. Shown as the blue line with an additional phase space contribution in green, a mass of 2117 MeV/c^2 and a width of 20 MeV/c^2 proved optimal. The higher energy broader peak is the reflection of the uncorrelated $\pi^0 d$ combination. The measured width is approximately the same as the experimental resolution and can therefore be considered an upper limit. This is much narrower than the width of 91 MeV/c^2 reported by the ELPH collaboration, which cannot be accounted for in this data and cannot give a satisfactory fit.

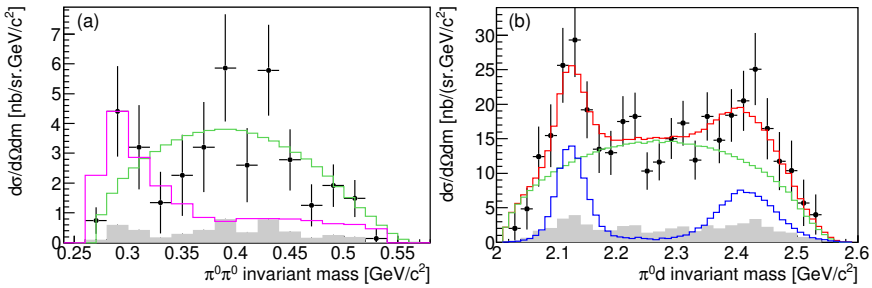

Figure 5. (a) The invariant mass of the $\pi^0\pi^0$ system for W from 2270 to 2441 MeV and $\cos\theta^d_{\rm CM} > 0.8$. The systematic uncertainties are the grey bars on the absisca. The green line is the phase space distribution with an integral equal to the measured data and the magenta line is the ABC effect distribution [21] with a scale fixed by the second data point at 0.29 GeV/c^2 (not the fit described in the text). (b) The invariant mass of the $\pi^0 d$ system for W from 2641 to 2696 MeV and $\cos\theta^d_{\rm CM} > 0.8$. The fitted distribution (red line) is comprised of phase space (green line) and the proposed sequential dibaryon decay (blue line). Figure adapted from Ref. [14].

The $\pi^0 d$ invariant mass for each W interval was fitted to extract the differential cross section of the proposed sequential decay shown as the blue squares in Fig. 4 (right). A Breit-Wigner function was fitted, and both the mass and width agrees with the proposed highest mass dibaryon from the ELPH collaboration. It is therefore suggested that two decay modes of an $N\Delta$ isoscalar dibaryon are observed, either directly to $\pi^0\pi^0 d$ or to $\pi^0\mathcal{D}_{12}$, where the $\mathcal{D}_{12}$ is an $N\Delta$ configuration dibaryon. Alternative explanations however can not be excluded at present, such as pion re-scattering mechanisms and may yet explain the observed spectra without the need for intermediate dibaryons.

4 Conclusions

The BGOOD experiment has very forward angle acceptance for charged baryons and mesons, and complemented by a central calorimeter ideal for neutral meson decay identification. This enables measurements at very low momentum exchange kinematics to recoiling hadron systems, which may be sensitive to molecular-like structure in the reaction mechanisms. The setup is currently being exploited to study strangeness photoproduction at low-t and to measure coherent meson photoproduction off the deuteron at forward angles.

Acknowledgements

This work is supported by the Deutsche Forschungsgemeinschaft Project Numbers 388979758 and 405882627, the Third Scientific Committee of the INFN and has received

funding from the European Union's Horizon 2020 research and innovation programme under grant agreement STRONG–2020 No. 824093.

References

[1] R. Aaij *et al.* (LHCb Collaboration), Phys. Rev. Lett. **122** 222001 (2019)
[2] Y.-R. Liu *et al.*, Prog. Part. Nucl. Phys. **107** 237 (2019)
[3] R. Ewald *et al.* (Crystal-Barrel@ELSA Collaboration), Phys. Lett. **B 713** 180 (2012)
[4] A. Ramos and E. Oset, Phys. Lett. **B 727** 287 (2013)
[5] S. Weinberg, Phys. Rev. **137** 672 (1965)
[6] S. Alef *et al.* (BGOOD Collaboration), Eur. Phys. J. **A 56** 104 (2020)
[7] W. Hillert, Eur. Phys. J. **A 28** 139 (2006)
[8] K. Kohl, T. C. Jude, *et al.* (BGOOD Collaboration), Eur. Phys. J. **A 59** 254 (2023)
[9] G. Scheluchin, T. C. Jude, *et al.* (BGOOD Collaboration), Phys. Lett. **B 833** 137375 (2022)
[10] S. Alef, *et al.* (BGOOD Collaboration), Eur. Phys. J. **A 57** 80 (2021)
[11] T. C. Jude *et al.* (BGOOD Collaboration), Phys. Lett. **B 820** 136559 (2021)
[12] C. S. Akondi *et al.* (A2 Collaboration), Eur. Phys. J. **A 55** 202 (2019)
[13] E. Wang *et al.*, Phys. Rev. **C 95** (2017) 015205 (2017)
[14] T. C. Jude *et al.* (BGOOD Collaboration), *Phys. Lett.* **B 832** 137277 (2022)
[15] P. Adlarson *et al.* (WASA-at-COSY Collaboration), Phys. Rev. Lett. **106** 242302 (2011)
[16] M. Bashkanov *et al.* (CELSIUS/WASA Collaboration), Phys. Rev. Lett. **102** 052301 (2009)
[17] N. E. Booth, A. Abashian and K. M. Crowe, Phys. Rev. Lett. **7(1)** 35 (1961)
[18] A. Fix and H. Arenhövel, Eur. Phys. J. **A 25** 115 (2005)
[19] M. Egorov and A. Fix, Nucl. Phys. **A 933** 104 (2015)
[20] T. Ishikawa *et al.* (ELPH Collaboration), Phys. Lett. **B 789** 413 (2019)
[21] P. Adlarson *et al.* (WASA-at-COSY Collaboration), Phys. Rev. **86 C** 032201 (2012)
[22] C. Garcia-Recio, M. F. M. Lutz and J. Nieves, Phys. Lett. **B 582** 49 (2004)
[23] M.-L. Du *et al.*, Phys. Rev. Lett. **124** 072001 (2020)